A Multifunction Series Inductive AC-Link Universal Power Converter with Reduced-Switch Count

Khalegh Mozaffari, Mahshid Amirabadi
Department of Electrical and Computer Engineering
Northeastern University
Boston, MA

***Abstract*—This paper proposes a new family of series inductive ac-link universal power converter with a lower number of switches compared to other series inductive ac-link universal converters. The number of switches in the proposed three-phase ac-ac configuration is reduced to 18; whereas, the original series inductive ac-link converter requires 24 switches. In this converter, the power is transferred from input to output entirely or partially through a small link inductor. A small capacitor that is placed in parallel with this inductor allows all the switches to benefit from zero-voltage switching (ZVS), which results in significant reduction of switching losses, stresses over the active switches, and electromagnetic interference (EMI). The converter structure enables an input voltage to be stepped up or down, and provides unidirectional power flow. This converter, in which the input and output can be dc, single-phase ac, or multi-phase ac, is capable of functioning in buck, boost, and buck-boost modes of operation. A combination of these operation modes is also feasible. Operating the converter in buck or boost functions leads to substantially decreased inductor link peak current, stress of the switches, and total power-loss compared to other inductive-link universal power converters. Galvanic isolation in the proposed converter can be provided by means of a compact lightweight single-phase high-frequency (HF) transformer connected to the link instead of a low-frequency transformer, which is a prominent contributor to size and weight of a conventional isolated converter. In view of these advantages, the proposed configuration offers improved efficiency, increased power-density, high reliability, reduced total cost, and wide range of operation in terms of input voltage. In this paper, the detailed behavior of the proposed converter is investigated, and performance of the converter is evaluated at various operating points through simulation and experimental results.**

Keywords—universal converter; partial-resonant converter, three-phase ac–ac converter; dc-ac converter; ac-dc converter; ac-link converter; zero-voltage switching

I. INTRODUCTION

Two-level back-to-back [1] and multilevel [2] dc-link converters are the most common types of ac-ac converters used for low and medium voltage industrial applications. However, the dc energy storage in the form of electrolytic capacitor is the main factor contributing to failure of these converters. As an alternative without an energy storage, matrix converters [3] are capable of providing bidirectional power flow, controllable input and output frequencies and power factors. However, this category of ac-ac converters suffer from limited voltage ratio, hard-switching, and commutation issues.

High-frequency (HF) link universal converters are an influential alternative solution for ac-ac or dc-ac power conversion. Special attention has recently been paid to soft-switched partial-resonant universal power converters due to their remarkable features including single-stage conversion, fast dynamic response, high efficiency, high reliability, step-up and step-down operations. A number of soft-switched universal power converter topologies have been reported in the literature. Soft-switched partial-resonant universal power converters are categorized as capacitive-link and inductive-link.

Capacitive-link universal converters are originally an extension of a Ćuk converter in which a link capacitor is the main energy component for transferring power from input towards output. This category of universal converters benefit from soft-switching operation via adding a small inductor in series with the capacitor link. In [4], a class of capacitive-ac-link power converters called series partial-resonant converter is proposed. To reduce the number of active switches, a modified configuration and a switching pattern, which can handle two-quadrant link, is proposed in [5].

In inductive link soft-switched partial-resonant universal converters the link is formed by a parallel ac inductor/capacitor pair, and the inductor is the main element of exchanging power between different ports of the system. In [6], a partial-resonant ac-ac power converter, which is originated from a buck-boost converter and is classified as an inductive-link universal converter, is presented. However, long resonating modes of this converter can degrade its performance, especially when a broad range of output voltages is required. To solve this issue, a modified configuration called parallel ac-link universal power converter, which has short resonating modes at the cost of doubling the number of active switches, is proposed in [7] and [8]. A number of reduced-switch configurations derived from this class of converter, which are called sparse [9], ultra sparse [10], and extremely sparse [11] parallel ac-link universal power converters, are introduced. Different applications of partial-resonant universal power converters are explored in electric vehicle [12], photovoltaic generation system [13], and electric drive [14]. The parallel inductive-link universal power converters proposed in [6]-[14] have large values of link peak current, which contributes to switch rating and power-loss of the system; therefore, they may face challenges for high power applications. To address this concern, two families of bidirectional universal power converter, which can function in buck, boost, and buck-boost modes of operation, are proposed in [15] and [16]. The topologies proposed in [15] take advantage of supporting four-quadrant link, which results in achieving better utilization of the link inductor and lower THD, compared to two-quadrant link configuration introduced in [16]. However, this degree of freedom is realized at the cost of using bidirectional switches, which can affect the reliability of the converter negatively, and increased control complexity.

To reduce the number of active switches and enhance reliability of topologies presented in [15], a new class of soft-switched HF ac-link universal power converter with reduced-switch count, which can function in buck, boost, and buck-boost modes of operation, is proposed in this paper. The proposed unidirectional configuration uses unidirectional switches and a series inductive-link for transferring power . In a three-phase ac–

ac configuration, the proposed converter can save six active switches compared to [15]. One of the advantages of the universal converters is that they can transfer power from multiple sources to multiple loads through a single-stage power conversion system. The potential advantage of the proposed converter in terms of reducing the number of active switches can be fully realized when the number of sources and loads is increased. Moreover, the proposed converter requires a simpler control algorithm to regulate input and output currents compared with control algorithm in [15]. This topology is expected to offer high efficiency and power density as a result of reduced link peak current, soft-switching operation, and possibility of adding a single-phase lightweight HF transformer for electrical isolation. Additionally, high reliability is granted to the proposed topology due to being electrolytic capacitor-less, reduced number of switches, reduced EMI, and being immune from short-circuit at the source and load terminals. Better utilization of the link inductor, decreased total harmonic distortion (THD), and supporting a wider range of input/output voltages are other advantages of this converter compared to inductive-link universal converters with non-alternating link inductor current.

Details of the proposed configurations, principle of the operation, and the control strategy are studied in sections II, III, and IV of this paper, respectively. In section V the proposed configuration and the topology introduced in [15] are compared in terms of component ratings and power-loss. Section VI presents simulation and experimental results. Finally, section VII concludes the paper.

II. Proposed Configurations

A family of the proposed converter is shown in Fig. 1. The proposed generic multi-phase m×n, three-phase ac–ac, and dc-to-three-phase ac configurations with an optional single-phase HF transformer are illustrated in Figs. 1 (a), (b), and (c), respectively.

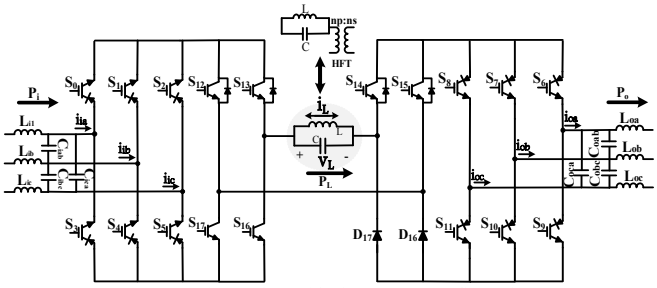

(a) Proposed generic multi-phase m×n configuration.

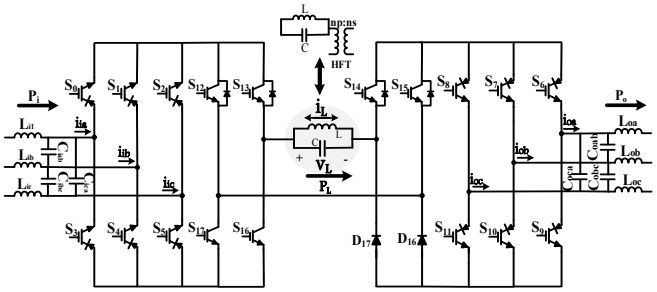

(b) Proposed three-phase ac–ac configuration.

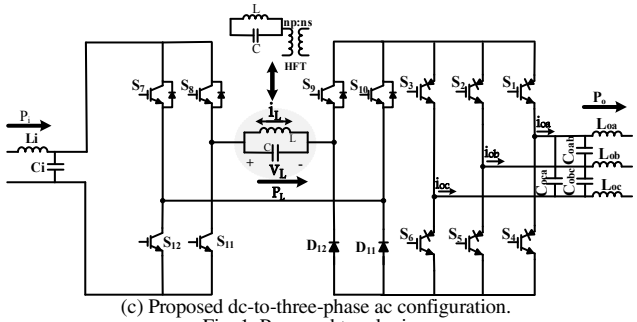

(c) Proposed dc-to-three-phase ac configuration.

Fig. 1. Proposed topologies.

In this converter, a small ac inductor L and a very small ac capacitor C form the HF ac-link. The proposed topology consists of an input switch-bridge, an output switch-bridge, and two switch-bridges called a link switch-bridge that connect the input and output switch bridges to the LC link and allow the inductor current to be alternating. The input and output switch bridges consist of forward-conducting bidirectional blocking switches, e.g. RB-IGBTs. The link switch bridge is composed of four forward-blocking and bidirectional-conducting switches, two forward-blocking and unidirectional-conducting switches, and two power diodes. Power is transferred from the input side to the output side partially or entirely via the link inductor, which is charged and discharged in both positive and negative directions. The proposed configuration can function in buck, boost, and buck-boost modes of operation. A combination of these modes of operation are also feasible, but it requires a complex control strategy due to multiple modes of operation and the resulting transitions between different modes.

III. Principles of Operation of Three-Phase AC-AC Converter

In this part, the principles of operation of the proposed three-phase ac-ac converter is studied. Principles of operation of the other proposed topologies are similar.

A. Overall Link Cycle Description and Assumptions

Fig. 2 illustrates a typical cycle of link voltage and current in the proposed three-phase ac-ac configuration. In each link cycle, the operation of the converter is divided into sixteen separate modes, including eight active modes and eight partial-resonant modes, which occurs alternately. Each link cycle includes charging and discharging the link inductor in both positive and negative direction, as shown in Fig. 2. The frequency of charging and discharging the link inductor in a complete cycle is called a link frequency, which is in general much higher than the input and output frequencies.

The references of phase currents and phase voltages change over the course of input and output ac cycles. To show the behavior of the converter in different modes of operation and functions, one link cycle is considered in this section. In this link cycle, it is assumed that the reference current of input phase c (i_{ic}^{*}) and the reference current of output phase b (i_{ob}^{*}) are both positive and have the highest absolute values of input reference currents i_{ia}^{*}, i_{ib}^{*}, i_{ic}^{*} and output reference currents i_{oa}^{*}, i_{ob}^{*}, i_{oc}^{*}, respectively. Additionally, it is considered that the voltage across input phase pair ca $|V_{ica}|$ is higher than $|V_{icb}|$, at the output side $|V_{oba}|$ is higher than $|V_{obc}|$, and the polarities of V_{ica}, V_{icb}, V_{obc}, and V_{oba} are all positive.

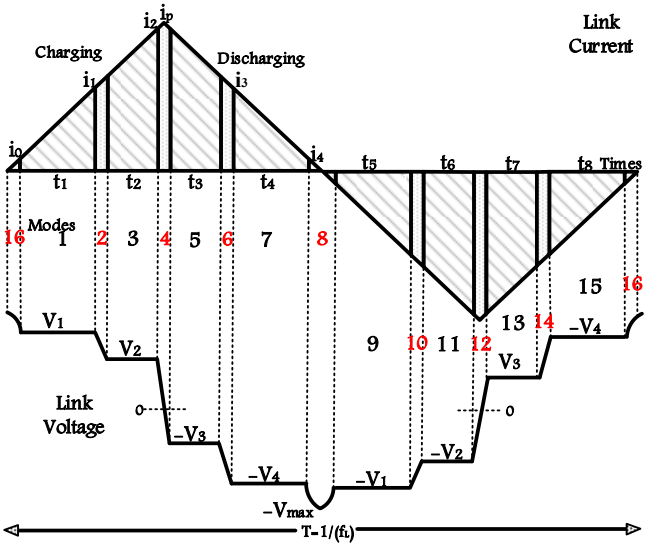

Fig. 2. A typical cycle of link voltage and link current in proposed three-phase ac-ac configuration.

B. *Behaviour of Mutifunction Converter*

Behavior of the proposed three-phase ac-ac converter in buck-boost, buck, and boost functions is demonstrated in Figs. 3-6.

Modes 1-4: Buck-Boost and Boost Functions: Switches S_2, S_3, and S_4 from the input switch-bridge and S_{13}, S_{15}, and S_{17} from the link switch-bridge are turned-on before starting mode 1, when the link voltage is higher than the input line-to-line voltages. Based on the assumption, switches S_2, S_3, S_{13}, S_{15}, S_{17} and diode D_{14}, start conducting when the link voltage becomes equal to $|V_{ica}|$, and this initiates mode 1. The link inductor is charged in mode 1, as demonstrated in Fig. 3(a), until the average of unfiltered current of phase a ($I_{avg,ia}$) meets its reference ($I^*_{avg,ia}$). Once this happens the switch corresponding to phase a, i.e. S_3, is turned-off. Then a resonating mode is initiated, and the link voltage starts decreasing until it reaches $|V_{icb}|$. At this time, switches S_2, S_4, S_{13}, S_{15}, S_{17} and diode D_{14} become forward-biased, and the inductor link is again charged but through phase pairs cbi, as illustrated in Fig. 3(b). Once the average of i_{ic} over half a cycle meets $I^*_{avg,ic}$, S_2, S_4, S_{13}, S_{15}, S_{17} are turned-off. This initiates another resonating mode, which is mode 4.

Modes 5-8: Buck-Boost and Buck Functions: During mode 4, the relevant switches at the output switch-bridge and the link switch-bridge are turned-on. Switches S_7, S_9, S_{11}, S_{13} and diodes D_{12}, D_{14} and D_{16} are activated at the beginning of mode 5 at zero-voltage to discharge the link inductor to the output phase pair bc, as shown in Fig. 4(a). This mode ends by turning off the switch S_{11} when the average current condition is satisfied for phase oc. Mode 6 as a resonating mode comes after this active mode during which the link voltage decreases. Once the link voltage reaches $|V_{oba}|$, the remaining switches that were turned on during mode 4 and along with diodes D_{12}, D_{14} and D_{16} become forward-biased to start mode 7, as demonstrated in Fig. 4(b). The link inductor continues to get discharged until the remaining stored energy in the link is only sufficient to swing the link voltage to a predetermined value called $-V_{max}$. Once the energy remained in the link reaches the determined limit, switches S_7, S_9, and S_{13} are all turned-off under zero-voltage-switching condition. Afterwards mode 8, as illustrated in Fig. 5 begins.

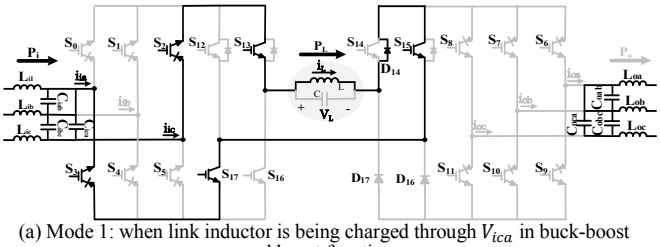

(a) Mode 1: when link inductor is being charged through V_{ica} in buck-boost and boost functions.

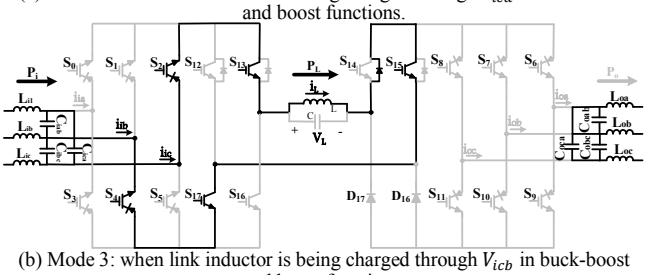

(b) Mode 3: when link inductor is being charged through V_{icb} in buck-boost and boost functions.

Fig. 3. Behavior of buck-boost and boost functions in modes 1 and 3.

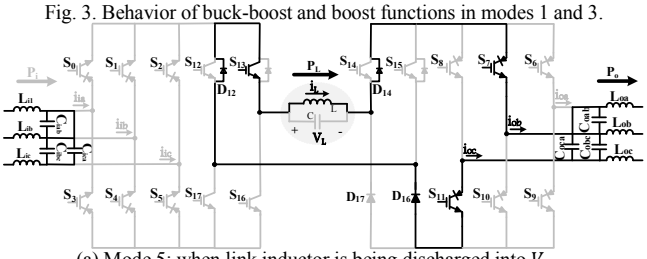

(a) Mode 5: when link inductor is being discharged into V_{obc}.

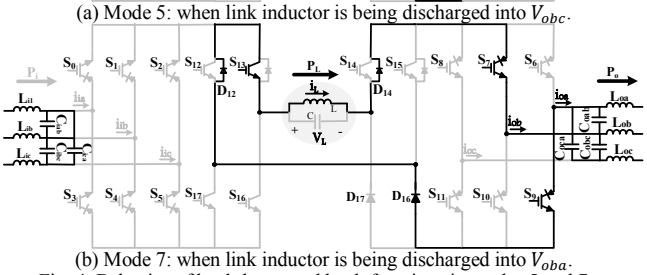

(b) Mode 7: when link inductor is being discharged into V_{oba}.

Fig. 4. Behavior of buck-boost and buck functions in modes 5 and 7.

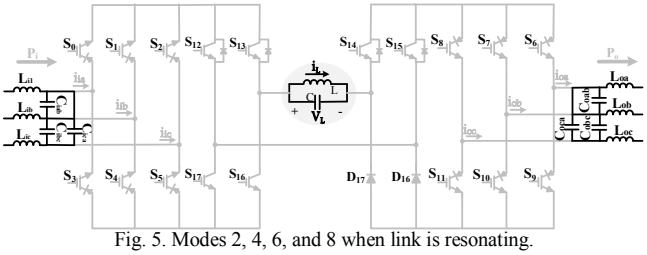

Fig. 5. Modes 2, 4, 6, and 8 when link is resonating.

Modes 1-4: Buck Function: Appropriate switches at the input and output switch bridges corresponding to the highest input and output line-to-line voltages along with switches S_{13}, S_{17} at the link switch-bridge are turned-on before mode 1. When switches S_2, S_3, S_7, S_9, S_{13}, and S_{17} become forward-biased, the input phase pair ca and output phase pair ba are connected to the link to charge the inductor, as depicted in Fig. 6(a). Voltage $V_{ica} - V_{oba}$, which is a positive voltage, is seen across the link inductor. This charging mode, mode 1, ends when $I_{avg,ia}$ is higher than $I^*_{avg,ia}$. At this moment, switches S_3, S_9 are turned-

off to initiate mode 2. Switches S_4 and S_{11} are also turned-on to connect the input and output phase pairs with the second highest line-to-line voltages to the link in mode 3. When mode 3, as shown in Fig. 6(b), starts, these switches are turned-on at zero voltage to charge the link inductor further. The link inductor is charged until the average current condition for input phase c is met, i.e. $I_{avg,ic} > I^*_{avg,ia}$. Once this happens, all the switches are turned-off to run another resonating mode, which is mode 4.

Modes 5-8: Boost Function: During mode 4, all proper switches that are supposed to conduct during modes 5 and 7 are turned-on. In this way, switches S_2, S_4, S_3 from the input switch-bridge, S_7, S_9, S_{11} from the output switch-bridge, and S_{13}, S_{17} from the link switch-bridge are turned-on. By turning on these switches, the voltage across the link during modes 5 and 7 can be: $V_{ica} - V_{oba}$, $V_{ica} - V_{obc}$, $V_{icb} - V_{oba}$, and $V_{icb} - V_{obc}$, which are all negative. According to the assumptions, switches S_2, S_3 corresponding to the input phase pair with higher line–to–line voltage (V_{ica}), and switches S_7, S_{11} corresponding to the output phase pair with lower line–to–line voltage (V_{obc}) automatically start conducting during mode 5 since they result in the lowest absolute value of voltage across the link. Mode 5, as illustrated in Fig. 6(c), begins as soon as the link voltage becomes equal to $V_{ica} - V_{obc}$, which is a negative voltage. During this mode the link voltage decreases. Mode 5 is over when the average of i_{oc} over half a cycle meets its reference. Turning off switches S_3 and S_{11}, introduces another resonating mode, mode 6. In mode 6, the link voltage again decreases until its value reaches $|V_{icb} - V_{oba}|$. Under this condition, switches S_2, S_4, S_7, S_9, S_{13}, S_{17} become forward-biased to discharge the link inductor into the output phase pair ba, while the input phase pair cb is also involved in transferring the power to the load, as shown in Fig. 6(d). This discharging mode is permitted to run until the reaming energy left in the link reaches a certain amount to peak the link voltage at $-V_{max}$.

The remaining modes, modes 9-16, are similar to modes 1-8 except that switches S_{12}, S_{14}, and S_{16} at the link switch-bridge have to be selected during modes 9-16 instead of switches S_{13}, S_{17}, and S_{15}, which are selected during modes 1-8, to charge and discharge the link inductor in a negative direction.

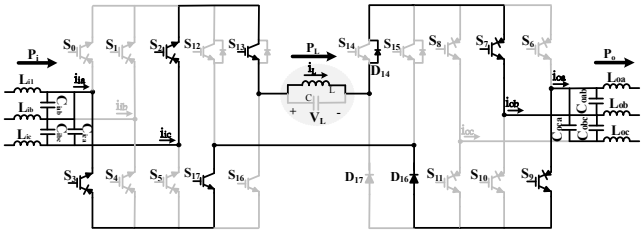

(a) Mode 1 in buck function: when link inductor is being charged from $|V_{ica} - V_{oba}|$.

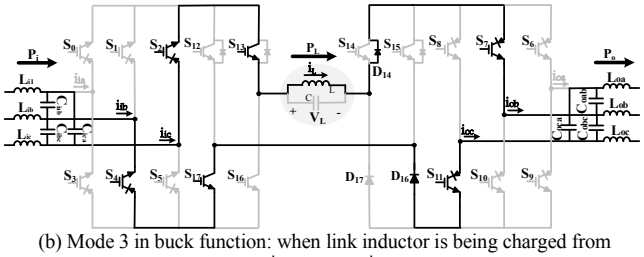

(b) Mode 3 in buck function: when link inductor is being charged from $|V_{icb} - V_{obc}|$.

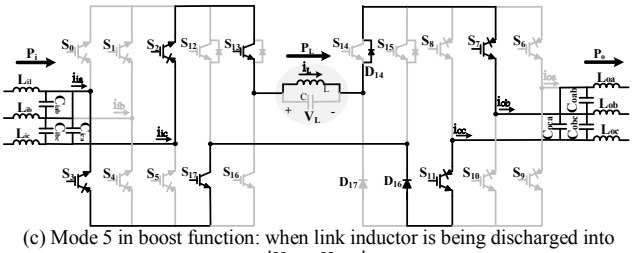

(c) Mode 5 in boost function: when link inductor is being discharged into $|V_{ica} - V_{obc}|$.

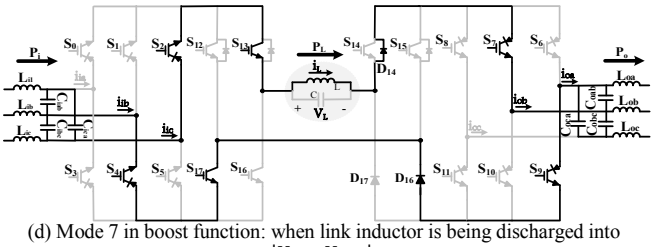

(d) Mode 7 in boost function: when link inductor is being discharged into $|V_{icb} - V_{oba}|$.

Fig. 6. Modes 1 and 3 in buck function and modes 5 and 7 in boost function.

Operating the converter in buck and boost functions leads to dramatically reduced link peak current, voltage and current ratings of the switches. In this soft-switched converter, the main source of power-loss is conduction loss of the switches and diodes and copper loss of the link inductor, which are determined based on the link peak current. In this way, lowering the link peak current in buck and boost functions increases the efficiency of the converter while reduces the ratings of switches.

IV. Soft-Switching Operation and Control Strategy

A. Zero-Voltage-Switching

In this converter, the proper switches are turned-on at the beginning of even modes, which are resonating modes, and the switches become forward-biased when the link voltage is equal to the selected voltage across the input phase pair, voltage across the output phase pair, or voltage difference of the input and output phase pairs. Therefore, the switches are turned-on at zero-voltage. Furthermore, when the switches are turned-off, an even mode is initiated. In this situation, the link voltage changes slowly, depending on the value of link capacitance. In this way, a zero-voltage-switching can also occur at the turn-off of the switches.

B. Overall Description of Control Strategy

The control strategy used in this converter is a closed-loop average current control, which is based on the comparison of average of measured unfiltered input and output currents, $I_{av,ia}$, $I_{av,ib}$, $I_{av,ic}$, $I_{av,oa}$, $I_{av,ob}$, and $I_{av,oc}$, and the average of input and output reference currents, $I^*_{av,ia}$, $I^*_{av,ib}$, $I^*_{av,ic}$, $I^*_{av,oa}$, $I^*_{av,ob}$, $I^*_{av,oc}$. Input and output current references are required to be determined in order to control the converter effectively. The input and output reference currents can be calculated based on the converter specification and an estimation of power-loss of the converter. Furthermore, the link voltage v_L and link current i_L are measured to determine the remaining stored energy in the link inductor for terminating modes 7 and 15 as well as polarity of the link inductor. Due to exclusion of any integrator, a faster dynamic response is expected, which can improve quality of regulated currents in general.

V. Comparison of Proposed Converter and Original Series Inductive AC-Link Universal Converter

In this section, similarities and differences of the proposed converter and the three-phase ac-ac topology presented in [15] in terms of component ratings and power-loss are detailed.

A. Link Component and Switch Ratings

The same design procedure presented in [15] can be followed to design the link inductor L and link capacitor C in the proposed configuration. Therefore, the rating of link components in the proposed converter is the same as that of converter proposed in [15]. The current stress of each switch can be determined by the maximum current passing through each switch, which is equal to the maximum link peak current, $I_{L,p}$. $I_{L,p}$ also dictates the power-loss of the converter. The voltage stress of the switches depends on the maximum value of the link voltage V_{max}. Thus, in this converter, it is desirable to decrease the maximum link peak current and maximum link voltage. V_{max} is slightly higher than the maximum line-to-line voltage. Although it depends on the link capacitance and inductance, it can be adjusted by the point at which modes 7 and 15 are ended. $I_{L,p}$ can be controlled by the link inductance and capacitance. Increasing the link inductance leads to lower maximum link peak current. On the other hand, increasing C results in slightly higher $I_{L,p}$. Furthermore, the value of link inductance L and capacitance C affect the link frequency f_L. Duration of active modes and resonating modes are decreased as the link inductance and the link capacitance decrease. As a result, the reduction of the link inductance and capacitance gives rise to increased link frequency, and consequently a compact design. In this way, depending on the required performance of the converter, a compromise should be made between the physical dimensions of the converter, power-loss, link frequency, and current stress of the switches to desirably design the link components.

The voltage stress of the switches/diodes in the proposed configuration can be determined as:

$$V_{S0-S5} = V_{S12,S13} = V_{S16,S17} = \max\left\{\sqrt{3}\times V_i, \frac{1}{4}(V_{\max} + 3\times V_i)\right\} \quad (1)$$

$$V_{S6-S11} = V_{S14,S15} = V_{D16,D17} = \max\left\{\sqrt{3}\times V_o, \frac{1}{4}(V_{\max} + 3\sqrt{3}\times V_o)\right\} \quad (2)$$

where V_i and V_o represents the peak values of input phase voltage and output phase voltage, respectively. The stress voltage of the switches in [15] can be calculated by:

$$V_{S0-S11} = \max\left\{\sqrt{3}\times V_i, \frac{1}{4}(V_{\max} + 3\times V_i)\right\} \quad (3)$$

$$V_{S12-S23} = \max\left\{\sqrt{3}\times V_o, \frac{1}{4}(V_{\max} + 3\sqrt{3}\times V_o)\right\} \quad (4)$$

The current stress of the switches/diodes ($I_{L,p}$) in the proposed converter and in [15] are the same. The average current passing through the switches located at input and output switch bridges is twice the average currents seen by non-shared input switches and output switches in [15], respectively. However, the average current tolerated by the switches at the shared input leg and the shared output leg in [15] is 1.66 times higher than that of the switches/diodes at the link switch bridge.

B. Power-Loss

The main source of power-loss in this converter is copper loss of the inductor and conduction loss of the switches. The switching losses are negligible since the converter benefits from ZVS. The copper loss of the inductor can be calculated as follows:

$$P_{cu} = \frac{1}{3}\times R_L \times I_{L,p}^2 \quad (5)$$

where R_L is the resistance of the link inductor. Since the link peak current and the link inductance in this converter are the same as in [15], the copper loss in both converters are the same. However, different conduction losses can be expected for the proposed converter and the converter proposed in [15] given that the average and rms currents of the semiconductor devices are different in these two converters. In this converter, in active modes of buck-boost function, modes 1, 3 of boost function, and modes 5, 7 of buck function, six semiconductor devices are involved. Whereas in modes 1, 3 of buck function, and modes 5 and 7 in boost function eight semiconductors conduct. In [15], regardless of functionality of the converter, eight semiconductor devices need to conduct. The conduction loss in this converter is higher than that of the topology presented in [15] when instead of reverse-blocking (RB) IGBTs, an IGBT in series with a diode are used as a forward-conducting reverse-blocking switch. However, RB-IGBTs, which offer lower on-voltage, are currently available in the market, and can be used in the proposed converter. For calculating the conduction loss in the proposed converter, switches S_0-S_{11} are considered to be RB-IGBTs.

The method presented in [17] is extended to estimate the conduction loss of the converter. For the three-phase ac-ac topology in [15], the conduction loss in buck-boost function $P_{c,BB}$ can be estimated by:

$$P_{c,BB} = \frac{3}{\pi}\times\left(4I_{i,\mathrm{p}} + 4I_{o,\mathrm{p}}\right)\left(V_{t,s} + V_{t,D}\right) + \frac{3}{2}\times\left(4I_{i,u}^2 + 4I_{o,u}^2\right)\left(r_{t,s} + r_{t,D}\right) \quad (6)$$

where $V_{t,s}$, $V_{t,D}$, $r_{t,s}$, $r_{t,D}$, $I_{i,p}$, $I_{o,p}$, $I_{i,u}$, $I_{o,u}$ are the IGBT threshold voltage, the diode threshold voltage, the IGBT series resistance, the diode series resistance, the peak of input phase current, the peak of output phase current, rms of unfiltered input phase current, rms of unfiltered output phase current, respectively. The conduction loss in the proposed converter using RB-IGBTs in buck-boost function can be calculated by:

$$\begin{aligned} P_{c,BB} = {} & \frac{3}{\pi}\times\left(5I_{i,\mathrm{p}} + 3I_{o,\mathrm{p}}\right)V_{t,s} + \frac{3}{2}\times\left(5I_{i,u}^2 + 3I_{o,u}^2\right)r_{t,s} \\ & + \frac{3}{\pi}\times\left(I_{i,\mathrm{p}} + 3I_{o,\mathrm{p}}\right)V_{t,D} + \frac{3}{2}\times\left(I_{i,u}^2 + 3I_{o,u}^2\right)r_{t,D} \end{aligned} \quad (7)$$

As it can be deduced from comparing (6) and (7), the conduction loss in the proposed converter is lower than that of converter proposed in [15].

VI. Simulation and Experimental Results

A. Simulation Results

In this part, a 20 kW three-phase ac-ac system with the input voltage of 440 V and the output voltage of 208 V is designed and simulated using PSIM software to step down. The link inductance and capacitance are selected as 30 µH and 20 nF to set the link frequency at 15 kHz for the given operating point. In this simulation, the capacitance and inductance of input and output filters are considered to be 5 µF, 40 µF, 40 µH and 50 µH.

Figs. 7-11 depict the simulation results corresponding to step-down operation in buck-boost function and buck function when the input and output frequencies are set at 60 Hz. The profile of the link current is shown in Fig. 7. As this figure

clearly demonstrates, the level of link peak current in buck-boost function is almost 1.5 times higher than of that in buck function, although the specifications of the system are the same. This shows that the power-loss in buck function is lower than that of in buck-boost function. The link current and voltage are depicted in Fig. 8. The maximum value of link current in buck-boost function and buck function are 213 A and 141 A, respectively. The maximum link voltage in buck-boost function is about 800 V, while this value in buck function is around 420 V. This implies that the voltage stress of the switches in buck function is expected to be much lower than that of buck-boost function. The unfiltered output currents are shown in Fig. 9. As it can be observed from this figure, the output phase pairs are involved in charging and discharging the link inductor in buck function, whereas in buck-boost function they only are responsible for discharging the link inductor. Fig. 10 depicts the output phase voltages with the peak value of 170 V. ZVS at turn-on of switch S_6 is demonstrated in Fig. 11.

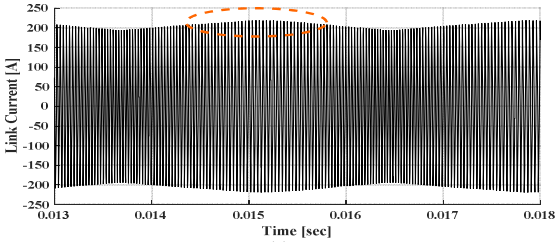

(a)

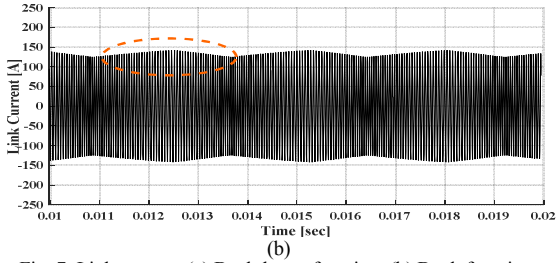

(b)

Fig. 7. Link current. (a) Buck-boost function. (b) Buck function.

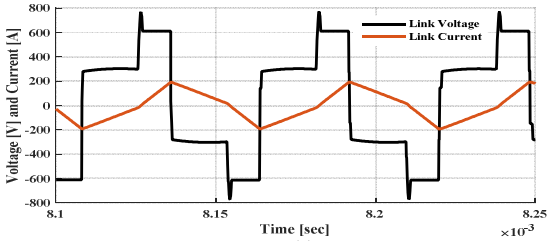

(a)

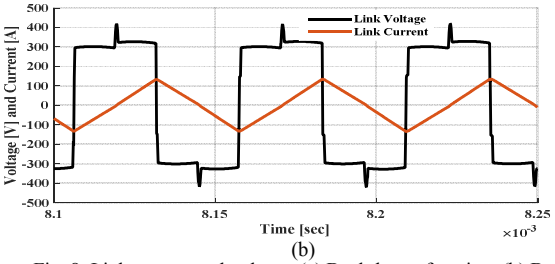

(b)

Fig. 8. Link current and voltage. (a) Buck-boost function. (b) Buck function.

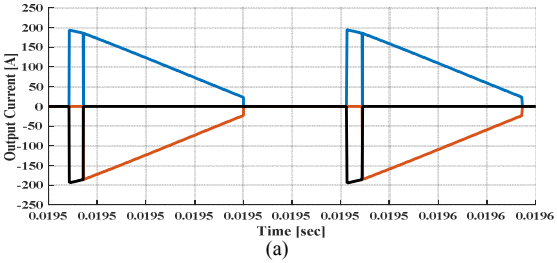

(a)

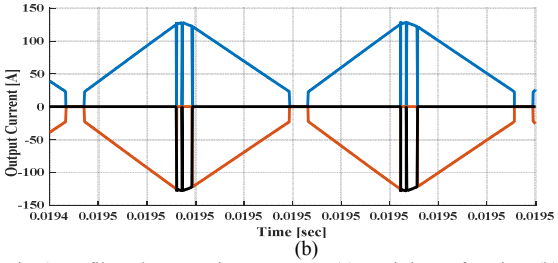

(b)

Fig. 9. Unfiltered output phase currents. (a) Buck-boost function. (b) Buck function.

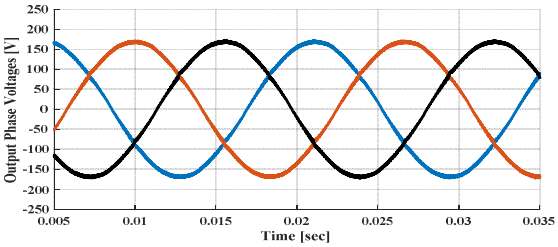

(a)

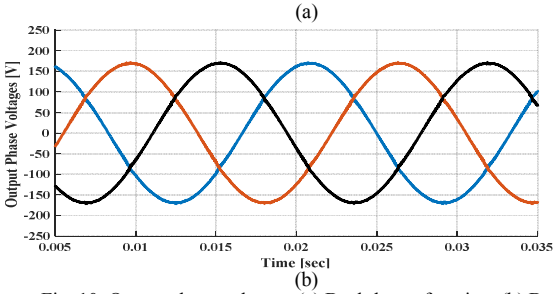

(b)

Fig. 10. Output phase voltages. (a) Buck-boost function. (b) Buck function.

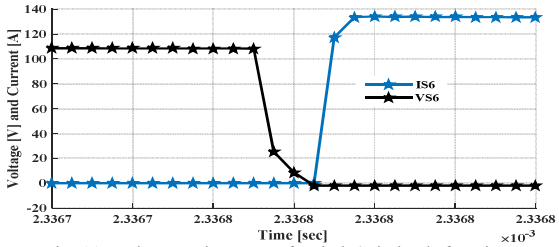

Fig. 11. Voltage and current of switch S_6 in buck-function.

Fig. 12 illustrates the filtered input and output phase currents when the frequency of source is set at 90 HZ in buck-boost function in the step-down operation. As it is clear from the figure, the input and output phase currents are well regulated at their reference values.

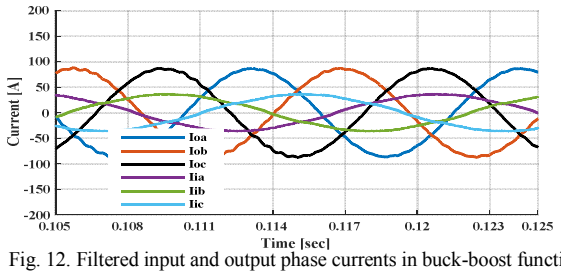

Fig. 12. Filtered input and output phase currents in buck-boost function.

B. *Exprimental Results*

A low power prototype is designed and fabricated to experimentally validate the performance of the proposed dc-to-three-phase ac converter topology. A TMS320F28335 Delfino digital signal processor (DSP) is employed with the sampling time of 5.5 μs to control the converter. In order to get sufficient samples in each link cycle, the link frequency is considered to be much smaller than the sampling frequency of DSP to run the converter properly. Accordingly, the link inductance and capacitance are selected as 785 µH and 700 nF, respectively. In this part, to verify and compare the performance of the converter in step-up and step-down operations in different functions, two sets of experiment are carried out.

Figs. 13-16 depict the experimental results corresponding to step-up operation in buck-boost function and boost function. In the first sets of experiment the converter is run with the dc input voltage of 61 V to supply a resistive 140V/60Hz 115 W load. Fig. 13 shows the filtered input dc current. The input current in both boost and buck-boost functions is well regulated at its reference value, which is 2.35 A. The link voltage and current are illustrated in Fig. 14. The maximum link voltages are 80 V and 125 V in boost function and buck-boost function, respectively. The link peak current is around 7.7 A in buck-boost function, while this current is 5 A in boost function. The load voltages with the peak value of 108 V are depicted in Fig. 15. Fig. 16 demonstrates the unfiltered output phase current carrying the maximum current in boost function. As it can be deduced from this figure, the output phases are only involved in discharging modes. The oscillations observed in the unfiltered currents are due to parasitic components of the switches and stray inductances of printed circuit board.

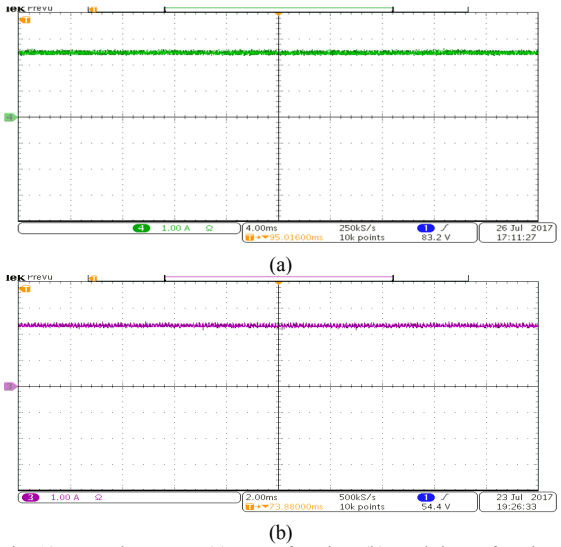
(a)

(b)

Fig. 13. Input dc current. (a) Boost function. (b) Buck-boost function.

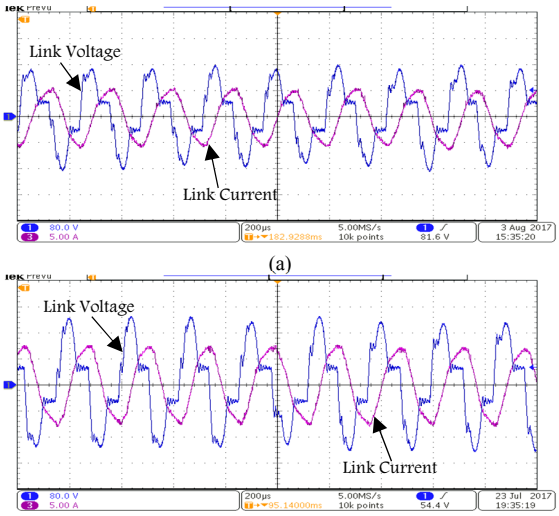

(a)

(b)

Fig. 14. Link voltage and current. (a) Boost function. (b) Buck-boost function.

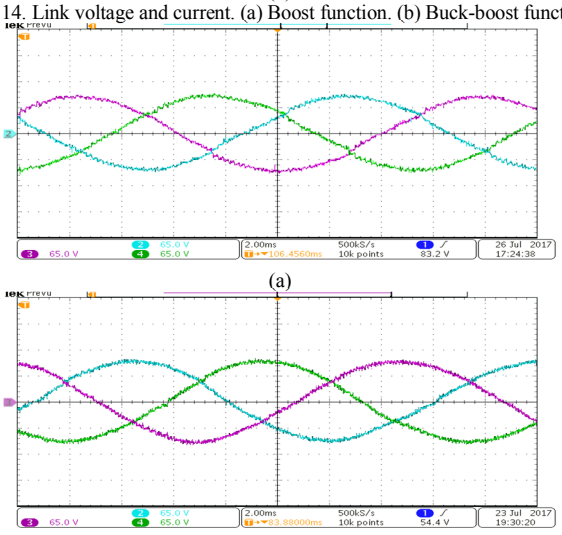
(a)

(b)

Fig. 15. Load phase voltages. (a) Boost function. (b) Buck-boost function.

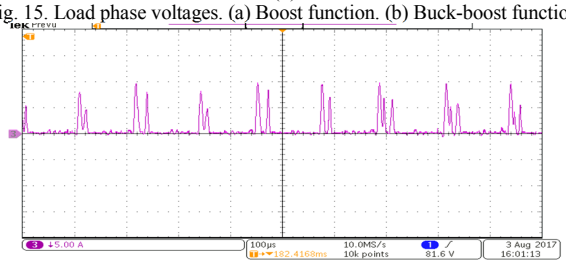
Fig. 16. Unfiltered input and output phase currents in boost function.

The second set of experiments is devoted to step-down operation of the converter. In this test, the input voltage is set at 92 V. Figs. 17-20 illustrate the experimental results of the step-down operation of the proposed converter in buck-boost function and buck function. The link voltage and link current are shown in Fig. 17. The average link frequency and link peak current in buck function are about 3.6 kHz and 3 A, respectively. The link frequency can be increased in order not to have audible noise, provided that a faster controller is used. As shown in Fig. 17, the link peak current in buck-boost function is twice that of buck function. The filtered input current and unfiltered current

corresponding to output phase carrying the maximum current in boost function are illustrated in Figs. 18 and 19, respectively. The dc current is set at 1.6 A. The load phase voltages in buck-boost function, the peak of which is 40 V, are depicted in Fig. 20.

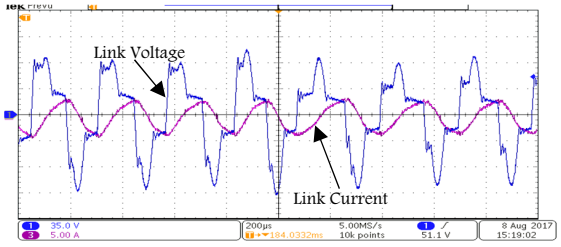

(a)

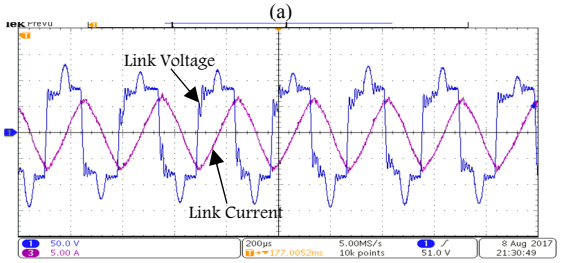

(b)

Fig. 17. Link voltage and current. (a) Buck function. (b) Buck-boost function.

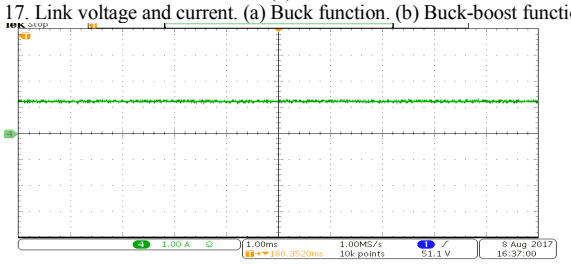

Fig. 18. Input current in buck function.

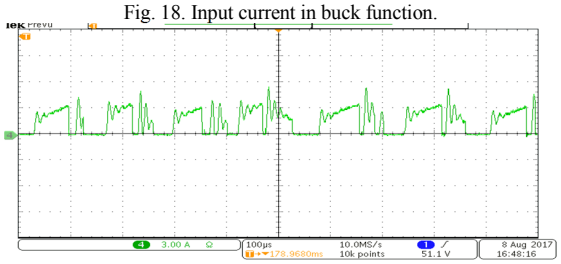

Fig. 19. Unfiltered output current in buck function.

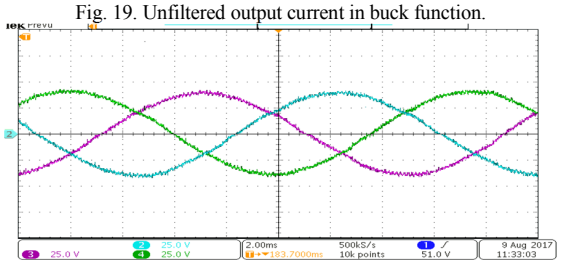

Fig. 20. Load phase voltages in buck-boost function.

VII. Conclusion

A new family of soft-switching inductive-link universal power converters with a reduced switch count is proposed in this paper. The proposed configuration can function in buck, boost, and buck-boost modes of operation to step up or down the input voltage. The buck and boost functions of the proposed unidirectional converter can dramatically reduce the link peak current, which makes this converter an appealing candidate for medium and high power applications. Galvanic isolation can be realized by adding a compact single-phase HF transformer to the link. The proposed soft-switched HF ac-link converter is expected to offer high reliability, efficiency, and power density, and can operate in a wide range of input/output voltages. As a universal converter, this converter can be configured as dc-to-ac, ac-to-dc, or ac-to-ac converters. Wind and PV generation systems are among numerous applications of the proposed converter. The simulation and experimental results verified the effectiveness and performance of the proposed converter in different functions.

References

[1] B. K. Bose, "Power electronics and motor drives recent progress and perspective", *IEEE Trans. Ind. Electron.*, vol. 56, no. 2, pp. 581–588, Feb. 2009.

[2] I. Colak, E. Kabalci, R. Bayindir, "Review of multilevel voltage source inverter topologies and control schemes," *Energy Convers Manage.*, vol. 52, no. 2, pp. 1114‑1128, Feb. 2011.

[3] T. Friedli, J. W. Kolar, J. Rodriguez, P. W. Wheeler, "Comparative evaluation of three-phase ac‑ac matrix converter and voltage dc-link back-to-back converter," *IEEE Trans. Ind. Electron.*, vol. 59, no.12, pp. 4487‑4510, Dec. 2012.

[4] M. Amirabadi, J. Baek, and H. A. Toliyat, "Bidirectional soft-switching series ac-link inverter," *IEEE Trans. Ind. Appl.*, vol. 51, no. 3, pp. 2312–2320, Oct. 2015.

[5] M. Amirabadi, "A new class of high-power-density universal power converter," in *Proc. IEEE ECCE'15*, Montreal, QC, 20-24 Sep., 2015, pp. 857-862.

[6] I. D. Kim, and C. Gyu-Hyeong, "New bilateral zero voltage switching ac/ac converter using high frequency partial-resonant link, " in *Proc. IEEE IECON'90*, Pacific Grove, CA, 2-6 Nov., 1990, pp. 857-862.

[7] W. C. Alexander, "Universal Power Converter," U.S. Patent US 2008/0 013351A1, Jan. 17, 2008.

[8] M. Amirabadi, J. Baek, H.A. Toliyat, and W.C. Alexander, "Soft-switching ac-link three-phase ac–ac buck–boost converter," *IEEE Trans. Ind. Electron.*, vol. 62, no.1, pp. 3–14, Jan. 2015.

[9] M. Amirabadi, J. Baek, and H. A. Toliyat, "Sparse ac-link buck-boostinverter," *IEEE Trans. Power Electron.*, vol. 29, no. 8, pp. 3942–3953, Aug. 2014.

[10] M. Amirabadi, H. A. Toliyat, and J. Baek, "Ultra-sparse ac-link converters," *IEEE Trans. Ind. Appl.*, vol. 51, no. 1, pp. 448–458, Jan./Feb. 2015.

[11] S.A.KH. Mozaffari Niapour, and M. Amirabadi, "Extremely sparse parallel ac-link universal power converters," *IEEE Trans. Ind. Appl.*, vol. 52, no.3, pp. 2456–2466, May/June 2016.

[12] S.A.KH. Mozaffari Niapour, and M. Amirabadi, "A highly reliable single-stage converter for electric vehicle applications," in *Proc. IEEE APEC'16*, Long Beach, CA, 20-24 Mar., 2016, pp. 3704-3711.

[13] M. Amirabadi, A. Balakrishnan, H. Toliyat, and W. Alexander, "High-frequency ac-link PV inverter," *IEEE Trans. Ind. Electron.*, vol. 61, no. 1, pp. 281-291, Jan. 2014.

[14] M. Amirabadi, H. Toliyat, and W. Alexander, "Partial resonant ac link converter: A highly reliable variable frequency drive," in *Proc. IEEE IECON'12*, Montreal, QC, 25-28 Oct., 2012, pp. 1946-1951.

[15] K. Mozaffari and M. Amirabadi, "A family of highly reliable and efficient inductive-link universal power converters," in *Proc. IEEE ECCE'17*, Cincinati, OH, 1-5 Oct., 2017, pp. 3462-3469.

[16] K. Mozaffari and M. Amirabadi, "A versatile inductive-link three-phase converter topology," in *Proc. IEEE ECCE'17*, Cincinati, OH, 1-5 Oct., 2017, pp. 3476-3483.

[17] M. Amirabadi, "Soft-Switching High-Frequency AC-Link Universal Power Converters With Galvanic Isolation," Ph.D. dissertation, Texas A&M Univ., College Station, TX, USA, 2013.